NE

NASA Technical Memorandum 81755

Electron Reflection and Secondary Emission Characteristics of Sputter-Textured Pyrolytic Graphite Surfaces

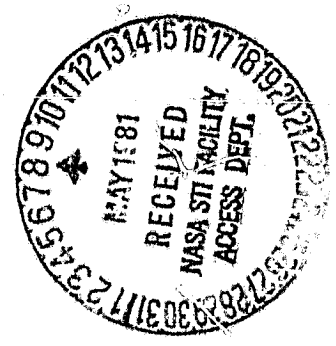

Edwin G. Wintucky, Arthur N. Curren, and James S. Sovey
Lewis Research Center
Cleveland, Ohio

(NASA-TM-81755) ELECTRON REFLECTION AND SECONDARY EMISSION CHARACTERISTICS OF SPUTTER-TEXTURED PYROLYTIC GRAPHITE SURFACES (NASA) 18 p HC A02/MF A01 CSCL 11D

N81-22193

Unclas
G3/27 42113

Prepared for the
International Conference on Metallurgical Coatings
sponsored by the American Vacuum Society
San Francisco, California, April 6-10, 1981

NASA

ELECTRON REFLECTION AND SECONDARY EMISSION CHARACTERISTICS OF SPUTTER-TEXTURED PYROLYTIC GRAPHITE SURFACES

by Edwin G. Wintucky, Arthur N. Curren and James S. Sovey

National Aeronautics and Space Administration
Lewis Research Center
Cleveland, Ohio 44135

E-818

1. INTRODUCTION

Broadband, high power traveling wave tube (TWT) microwave amplifiers are used in military electronic countermeasure and communications satellite applications where high electrical power efficiency is an important requirement. Electron beams with energies on the order of 10 keV are used to amplify the microwave signals. The electrical efficiency of a TWT is substantially improved by the use of a multistage depressed collector (MDC), which is a stack of axisymmetric electrode plates designed to usefully recover part of the kinetic energy of the electron beam at the output end of the TWT.[1,2] Electrons entering the MDC are slowed by a retarding electric field and strike the collector plates at reduced energies which are experimentally observed to be generally in the range of 500 to 1000 eV. The overall TWT efficiency depends strongly on the collector efficiency. An important factor influencing collector efficiency is the effectiveness of the electrode surfaces in absorbing electrons. Significant energy losses can occur through emission of electrons from the surface as a result of electron bombardment. The electron emission process is quite generally called secondary electron emission and includes both electrons reflected elastically without loss of energy (reflected primaries) and electrons which undergo inelastic collisions with the lattice and are emitted at lower energies (true secondaries). Reflected primary electrons generally constitute 5 to

10 percent of the secondary electron emission. A measure of secondary electron emission is the secondary electron emission yield, δ, which is usually defined as the ratio of the total number of emitted electrons to the number of incident primary electrons. For large electron absorption and consequently optimum collector efficiency, one obviously needs collector electrode surfaces with low secondary electron emission yields.

Because of its good mechanical, electrical and thermal properties, copper (Cu) has been widely used for collector electrodes, although Cu is not a particularly low emitter of secondary electrons. Two methods currently of interest for reducing the secondary electron emission of copper electrodes are roughening the surface and coating the surface with titanium carbide (TiC).[4] Roughening the surface, especially on a microscopic scale, provides recesses for trapping emitted electrons and thereby reduces the measurable emission. A microscopic cone structure produced by argon ion beam sputter texturing has been shown to effectively reduce secondary electron emission from Cu surfaces. TiC has an inherently lower secondary electron emission than Cu, which is further reduced by the natural roughness of sputter deposited TiC coatings.

Soot (carbon black) is one of the lowest known secondary electron emitting materials. Soot has poor adhesion and lacks the mechanical integrity necessary for space applications. However, carbon in the form of pyrolytic graphite (PG) is very attractive as a collector electrode material for space applications. PG is a relatively light weight, mechanically strong material with suitable electrical properties and has both high planar thermal conductivity and high thermal emittance for the enhancement of collector cooling. A previous study demonstrated that a microscopic needle-like surface structure produced by argon ion beam sputter-texturing further

reduced the secondary electron emission of PG to levels near those of soot.[4] This paper describes the secondary electron emission and reflected primary electron characteristics of pyrolytic graphite for distinctly different surface microstructures resulting from variation of the argon ion sputter-texturing parameters.

2. SPUTTER-TEXTURING OF PYROLYTIC GRAPHITE

The pyrolytic graphite (PG) samples consisted of circular discs, 21 mm in diameter and 2 mm thick. The PG crystalline orientation was the same as for collector electrode applications with the flat surfaces parallel to the direction of high strength and high thermal conductivity (the "a" direction). Surfaces to be sputter-textured were initially in a vapor-deposited condition. A few samples were scraped clean and retextured. Figure 1(a) shows a scanning electron microscope (SEM) photograph of an untextured PG surface. All PG was of high purity with a maximum 0.01 percent ash content as determined in combustion tests.

Pyrolytic graphite develops a natural surface texture under ion bombardment without requiring seeding material. The sputter-texturing parameters are ion energy, ion current density and sputter duration. Their values depend on which argon ion bombardment technique is employed.

One PG sample was sputter-textured for 13.7 hours in a radio frequency (RF) generated plasma at an average argon ion energy of 1800 eV and a current density of approximately 0.7 mA/cm^2. The resulting surface microstructure, shown in Fig. 1(b), consists typically of scattered clumps of micron-size toothlike protuberances.

In a second technique, the PG surfaces were sputter-textured by a normally incident 750 eV ion beam from a 30 cm-diameter argon ion source.[5] A short exposure to the ion beam of 0.5 hours at an ion current density of

1.1 mA/cm^2 produces a surface microstructure consisting of a dense array of uniformly-sized small cones (Fig. 1(c)). A longer exposure of 4.6 hours also at 1.1 mA/cm^2 produces a noticeably different cone structure (Fig. 1(d)) in which the cones are of much larger size, randomly distributed and of varying peak heights (on the order of microns). Ion beam sputter-texturing for 4.7 hours at a lower ion current density of 0.5 mA/cm^2 results in a similar cone-like microstructure but with the cones both smaller and less clustered.

Both the ion beam and RF plasma techniques necessitated that sputter-texturing be performed at low ion current densities (1.1 mA/cm^2 or less). Because PG is an inherently low sputter yield material, the corresponding sputter-etch rates were low.

To enhance the sputter-etch rate, the 30-cm diameter argon ion source was converted to a DC triode sputtering configuration[6] which enables much higher ion current densities. In this approach, the ion beam focus grids are replaced by an electrically isolated plate with an orifice having nearly the same geometry as the PG sample holder. The PG target is then biased negative relative to the discharge plasma potential. Ion current densities of 5 mA/cm^2 are readily obtained in this manner with current densities of 10 mA/cm^2 or higher possible. The PG samples were sputter-textured at ion energies of 500 and 1000 eV. The high ion current density (5 mA/cm^2) bombardment produces a much more dense cone-like microstructure than the low current density techniques. The structure produced at 500 eV consists of tall slender cones or spires randomly distributed in a dense background of smaller cones. Varying the etch time from 4 to 19 hours does not significantly alter the PG surface microstructure. The microstructure shown in the SEM photograph in Fig. 1(e) is representative of that sputter-etched at

500 eV (5 mA/cm^2, 4 hr). At 1000 eV, the structure is a more uniform, dense array of tall, thin spires ($\leq$1 μm diam, 5-10 μm high) and appears similar for etch times of 6 and 18.5 hours. Shown in the SEM photograph of Fig. 1(f) is a typical example of the microstructure resulting from sputter-etching at 1000 eV (5 mA/cm^2, 6 hr).

3. ELECTRON EMISSION CHARACTERISTICS

Measurements of secondary electron emission and reflected primary electron characteristics were made with an Auger cylindrical mirror analyzer[4] in a high-vacuum chamber at pressures below 1.33×10^{-7} N/m^2 (10^{-9} torr). The primary electrons were normally incident on the sample surface at energies ranging from 200 to 2000 eV.

Surface contaminants, such as absorbed gaseous impurities, can significantly alter the secondary electron emission levels.[4] To ensure clean surfaces, it is necessary to first bake out the samples. The PG samples were heated to temperatures above 850° C both by resistance heaters mounted on the sample holder and by electron bombardment. Temperatures were monitored by a Pt-13 percent Rh/Pt thermocouple embedded inside the PG disk. A residual gas analyzer indicated when the surfaces were free of gaseous impurities.

Soot (carbon back) has exceptionally reproducible secondary electron emission characteristics and is useful as a standard, control surface. One half of each PG disk was coated with soot after careful removal of the sputter texture. Measurements of electron emission characteristics were made successively on both soot and the test surface during the same run. Figure 2 shows an untextured PG disk, half of which is coated with soot, mounted in the sample holder.

The secondary electron emission yield, δ, defined as the ratio of secondary electrons emitted to primary electrons incident per unit time, is experimentally determined for a given primary energy, E_p, from measurements of the primary electron current, I_p, and the current passing through the sample to ground, I_T, according to

$$\delta(E_p) = \frac{I_p - I_T}{I_p}$$

The quantity $I_p - I_T$ is the total emitted secondary electron current, which is collected by the surrounding grounded vacuum chamber.

The reflected primary electrons are detected by an energy analyzer technique in which only those electrons emitted with energies equal to the primary electron energy are selectively focused and collected. The resulting analyzer output signal, although representative of the magnitude of the reflected primary electron current, is not by itself meaningful unless it is indexed relative to similar measurements with a standard surface. A useful parameter, which enables a meaningful comparison between the reflected primary electron characteristics of various surfaces, is the "reflected primary electron index," defined here as the ratio of the analyzer output signal amplitude for the test surface at a given primary energy to that for soot at a primary energy of 1000 eV.

The composite photograph in Fig. 1 shows the previously described surface textures arranged in order of apparent height and density of microstructure, with the untextured PG surface (1(a)) at one end and the dense, tall spire-like structure (1(f)) at the other. These textured surfaces are representative of the notably different surface microstructures produced by argon ion bombardment in the work reported here. Figure 3 is a plot of secondary electron emission yield, δ, versus primary electron energy, E_p,

for the six surfaces shown in Fig. 1. For comparison, a typical δ vs. E_p curve for soot is also presented. Figure 4 is a plot of the reflected primary electron index, π, versus primary electron energy, E_p, for the same surfaces as in Fig. 3.

The emission characteristics, δ and π, in Figs. 3 and 4 correlate well with the height and density of the surface microstructures shown in Fig. 1. In progressing from the relatively smooth surface of untextured PG in Fig. 1(a) to the dense, tall spire-like structure in Fig. 1(f), δ and π are in general correspondingly reduced. The higher and denser microstructures appear to provide more effective electron traps.

For $E_p < 1000$ eV, all of the sputter-textured surfaces reduce δ and π below that of untextured PG. For $E_p > 1000$ eV, both δ and π for the sparse structure of Fig. 1(b) are about equal to or slightly greater than for untextured PG. The δ for the surface with the small cone structure (Fig. 1(c)) is about the same as for untextured PG for $E_p > 1000$ eV, but π is somewhat reduced.

For $E_p < 500$ eV, the measured δ for both surfaces in Figs. 1(d) and (e) is approximately the same as for soot, whose electron emission characteristics are among the lowest observed for any material. The π for surface 1(d) is slightly less than that of soot whereas π for surface 1(e) is slightly more. Both surfaces 1(d) and (e) have some tall cone-like microstructure. For E_p in the range of 500 to 1000 eV, the measured δ and π for both surfaces are approximately equal to or lower than for soot. For $E_p > 1000$ the same two surfaces, 1(d) and (e) have δ lower than soot, whereas π is nearly equal to or slightly greater than soot.

Both δ and π for the surface with the dense, tall spire-like microstructure (Fig. 1(f)) are well below those of soot over the entire range of

E_p. In the primary electron energy range of 500 to 1000 eV, which is of considerable interest for TWT collector applications, sample 1(f) shows reductions in δ and π of at least 45 and 83 percent, respectively, when compared to untextured PG.

Figures 5 and 6 show the δ and π curves for five materials, pure, smooth Cu,[4] sputter-deposited TiC on Cu,[4] untextured PG, soot and textured PG (Fig. 1(f)). Cu and TiC on Cu are presently used for collector electrodes. For E_p = 1000 eV, π is above 40 for smooth Cu, about 10 for TiC and only 0.5 for textured PG. At the same E_p, δ is almost 1.1 for smooth Cu, about 0.55 for TiC and approximately 0.3 for textured PG. Sputter-textured PG, with its superior electron emission characteristics, is thus a very promising collector electrode material for TWT microwave amplifier applications.

4. CONCLUSIONS

The results of this study clearly demonstrate that sputter texturing effectively suppresses secondary electron emission from pyrolytic graphite surfaces. A dense, tall, thin spire-like microstructure, readily obtained at ion energies of 1000 eV and ion current densities of 5 mA/cm^2, is the most effective. The secondary electron emission from such a surface is observed to be lower than that of soot, whose secondary emission is among the lowest of any material. At a primary electron energy of 1000 eV, the secondary electron emission yield of smooth Cu is about 350 percent greater than the lowest value obtained for sputter-textured PG. The reflected primary electron index of smooth Cu is a factor of 80 greater. If the secondary electron emission yield is reduced to 0.3, which certainly appears possible with sputter-textured PG, the TWT collector efficiency could be

improved by as much as 4 percent over that for smooth copper. Calculations show this could result in at least a 12 percentage point gain in overall efficiency of the TWT microwave amplifier,[7] which is a substantial improvement.

5. REFERENCES

1. H. G. Kosmahl, NASA Tech. Note TN D-6093, 1971.
2. P. Ramins and T. A. Fox, NASA Tech. Publ. TP-1670, 1980.
3. D. J. Gibbons, in A. H. Beck (Ed.), Handbook of Vacuum Physics, Vol. 2, Part 3, Permagon Press, New York, 1966, p. 301.
4. R. Forman, NASA Tech. Publ. TP-1097, 1977.
5. J. S. Sovey, AIAA Paper No 76-1017, Nov. 1976.
6. E. G. Wintucky, et al., AIAA Paper No. 81-671, Apr. 1981.
7. P. Ramins, H. G. Kosmahl, and T. A. Fox, NASA Tech. Memo TM X-73486, 1976.

FIGURE CAPTIONS

Figure 1. - Sputter-textured pyrolytic graphite surfaces (a) untextured, (b) RF plasma - 1800 eV, 0.7 mA/cm^2, 13.7 hr, (c) ion beam - 750 eV, 1.1 mA/cm^2, 0.5 hr, (d) ion beam - 750 eV, 1.1 mA/cm^2. 4.6 hr, (e) triode plasma - 500 eV, 5 mA/cm^2, 4 hr, (f) triode plasma - 1000 eV, 5 mA/cm^2, 6 hr.

Figure 2. - Pyrolytic graphite disk mounted in sample holder.

Figure 3. - Secondary electron emission yields of sputter-textured pyrolytic graphite surfaces.

Figure 4. - Reflected primary electron indices of sputter-textured pyrolytic graphite surfaces.

Figure 5. - Secondary electron emission yield as a function of primary electron energy.

Figure 6. - Reflected primary electron index as a function of primary electron energy.

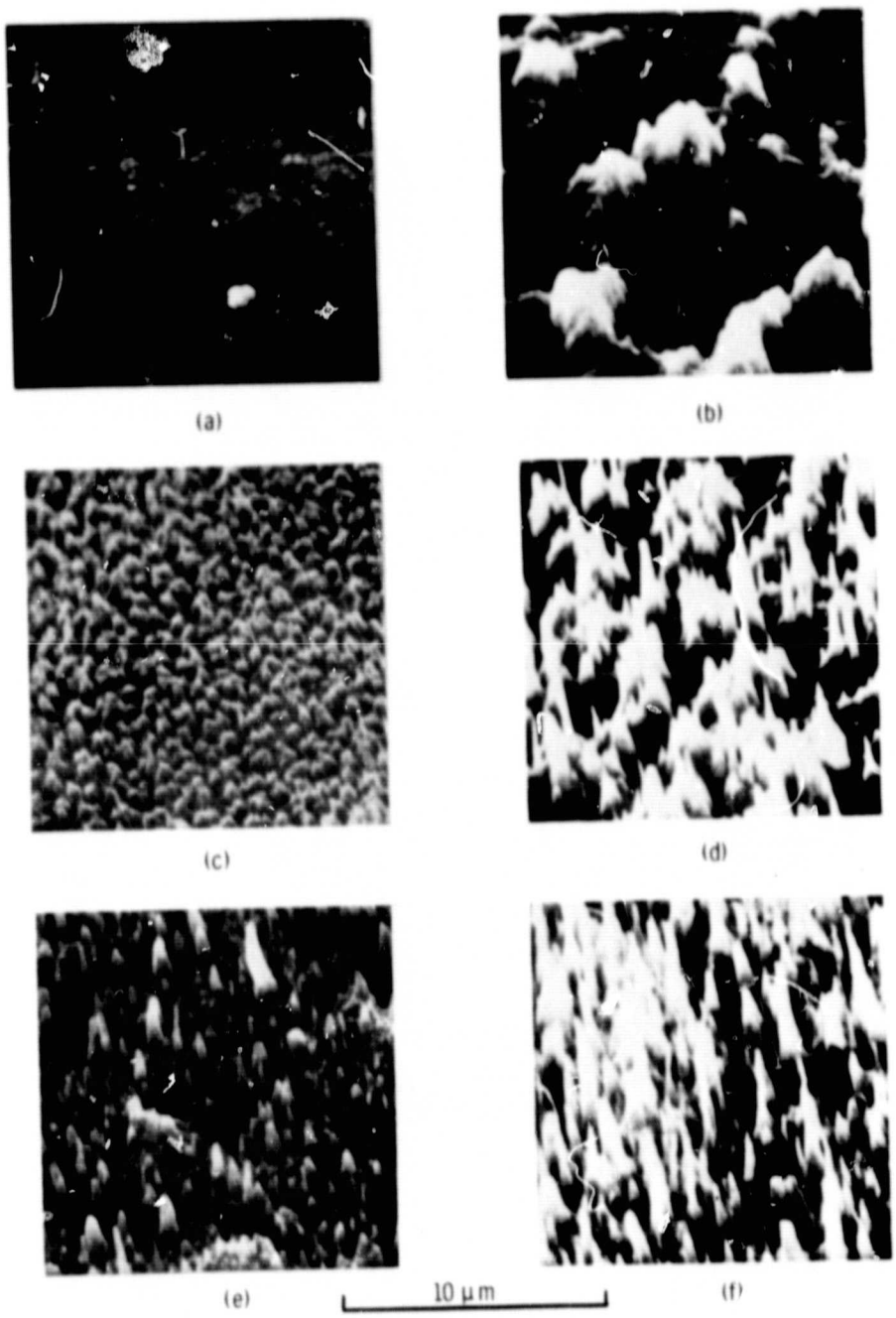

Figure 1. - Sputter-textured pyrolytic graphite surfaces (a) untextured, (b) RF-plasma 1800 eV, 0.7 mA/cm^2, 13.7 hr, (c) ion beam - 750 eV, 1.1 mA/cm^2, 0.5 hr, (d) ion beam - 750 eV, 1.1 mA/cm^2, 4.6 hr, (e) triode plasma - 500 eV, 5 mA/cm^2, 4 hr, (f) triode plasma - 1000 eV, 5 mA/cm^2, 6 hr.

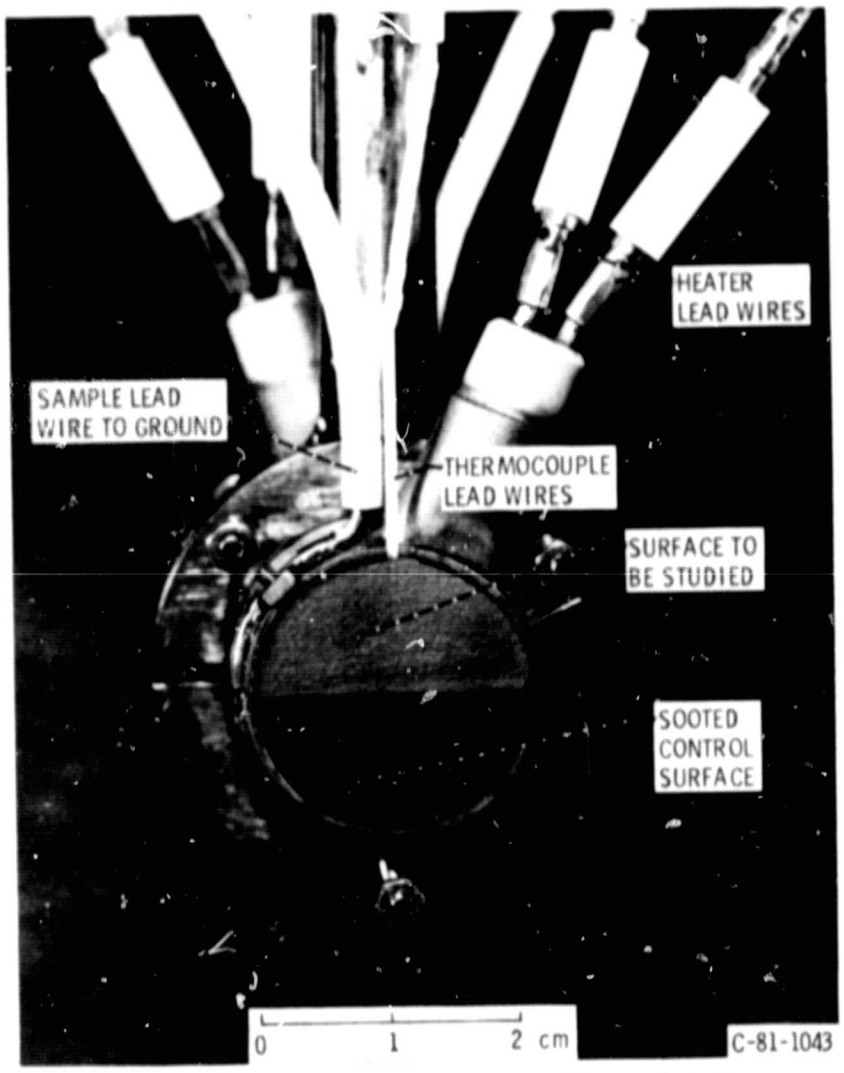

Figure 2. - Pyrolytic graphite disk mounted in sample holder.

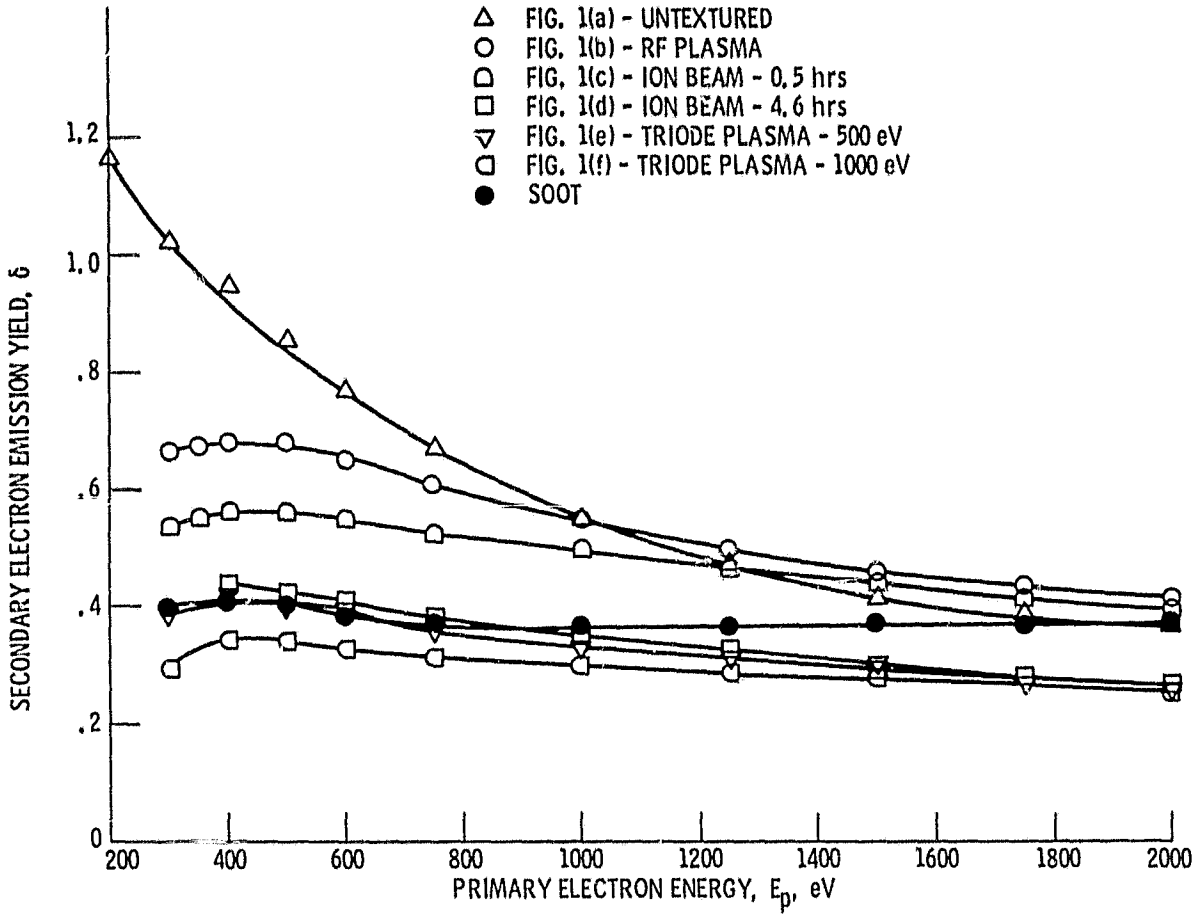

Figure 3. - Secondary electron emission yields of sputter-textured pyrolytic graphite surfaces.

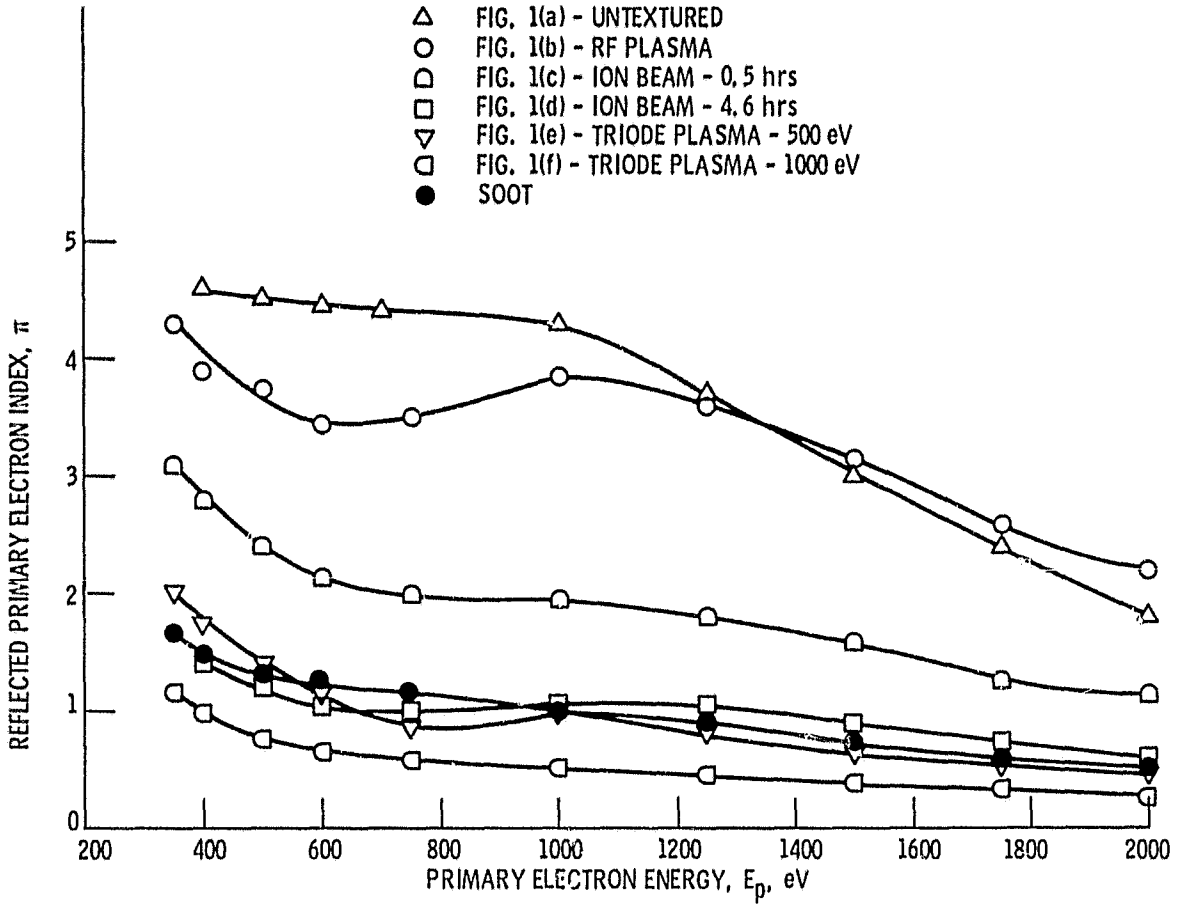

Figure 4. - Reflected primary electron indices of sputter-textured pyrolytic graphite surfaces.

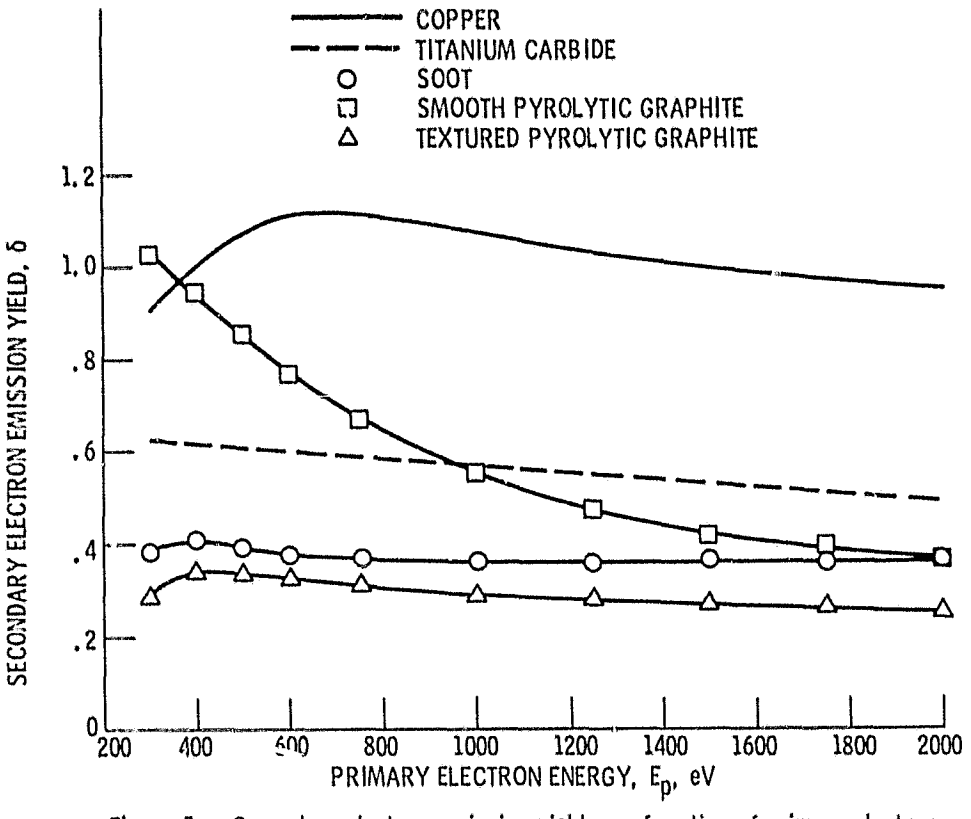

Figure 5. - Secondary electron emission yield as a function of primary electron energy.

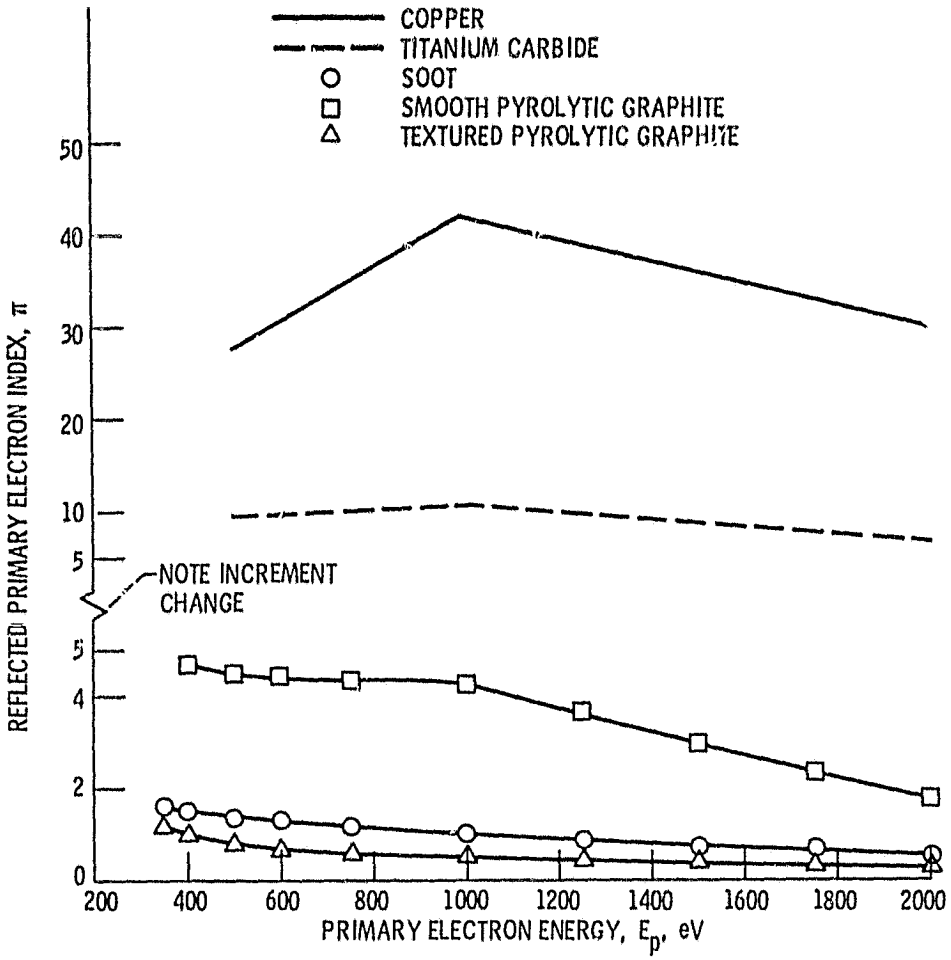

Figure 6. - Reflected primary electron index as a function of primary electron energy.